Catalysis Today 165 (2011) 25–31

Contents lists available at ScienceDirect

Catalysis Today

journal homepage: www.elsevier.com/locate/cattod

Does confinement effect always enhance catalytic activity? A theoretical study of H_2 dissociation on CNT supported gold clusters

Zhe Li [a], Zhao-Xu Chen [a,*], Guo-Jun Kang [a], Xiang He [a,b]

[a] Institute of Theoretical and Computational Chemistry, Key Laboratory of Mesoscopic Chemistry of MOE, School of Chemistry and Chemical Engineering, Nanjing University, Hankou Road 22#, Nanjing 210093, Jiangsu, People's Republic of China
[b] Eco-Materials and Renewable Energy Research Center, Department of Physics, Nanjing University, Nanjing 210093, People's Republic of China

ARTICLE INFO

Article history:
Received 14 September 2010
Received in revised form
23 November 2010
Accepted 25 November 2010
Available online 28 December 2010

Keywords:
Gold cluster
Carbon nanotube
H_2 dissociation
Confinement effect

ABSTRACT

Density functional theory (DFT) calculations are performed to investigate the interactions of small Au_n (n = 1–5) clusters with single-walled carbon nanotubes (CNTs) and H_2 dissociation on the CNT supported clusters. Encapsulated Au clusters interact more strongly with the metallic CNTs than with the semiconducting ones, where charge transfers from CNTs to the clusters play an important role. The clusters deposited outside the CNT are more stable than the ones encapsulated inside the tubes except for Au_1 and Au_3 on CNT(6, 6). Generally H_2 dissociation becomes more favorable thermodynamically, especially on the encapsulated clusters. Except for Au monomer, H_2 dissociation on the encapsulated clusters is kinetically more difficult than on the outside deposited clusters. Compared with the situation on bare clusters, H_2 dissociation needs to overcome higher barriers on CNT supported clusters, apart from that on Au monomer on the outer surface of the CNTs and on the encapsulated Au dimer. These kinetic results demonstrate that confinement effect is not helpful for all reactions and CNT supported catalysts do not improve the activity for all reactions.

1. Introduction

Carbon nanotubes (CNTs) have a series of properties such as high surface area, special size and hollow geometries and unique physical morphology, which make them attractive supports for heterogeneous catalysts [1–3]. Among various properties, confinement effect induced by the channel structure of CNTs seems most salient, and enhancement of catalytic activity and/or selectivity due to this effect is often reported. It is observed that the C=O bond of cinnamaldehyde is hydrogenated highly selectively on platinum particles encapsulated in the CNTs while on Pt deposited outside the CNTs both C=C and C=O bonds are completely hydrogenated [4]. Bao et al. found that the encapsulated Fe/Fe_2O_3 in the carbon nanotube significantly improved the activity to Fisher–Tropsch synthesis [5], and they also reported enhanced ethanol production from CO and H_2 catalyzed by Rh particles confined inside nanotubes [6]. The catalytic activity enhancement is attributed to the effect of confinement of the catalysts within the CNT channels [5,6]. Very recently it is demonstrated that the sintering of the Co/carbon catalysts deposited on the inner sides of the CNTs is more difficult compared with the particles located on the outer layers of the CNTs, likely due to the difference in electronic properties between inner and outer surfaces of CNTs and confinement effect [7].

As far as we know, positive aspects of confinement effect on catalysis are reported and there is no report on the negative influence of confinement effect. In the present paper, by investigating H_2 dissociation on CNT supported gold clusters we demonstrated that the confinement effect is not helpful for all reactions and CNT supported catalysts do not improve the activity for all reactions. We chose H_2 dissociation as probe reaction because it is usually the first step of hydrogenation reaction, and often used as a model system to probe the activity of metal catalysts. In addition, it is computationally less expensive. We selected "catalytically inert" metal gold as catalyst because since the work of Haruta et al. [8] and Hutchings [9], gold is found to exhibit activity for various reactions like low temperature CO oxidation [10–12], hydrogenation of α, β-unsaturated aldehyde [13], water gas shift reaction [14], epoxidation of propene [15], oxidation of alcohols and aldehydes [16,17] and the direct synthesis of H_2O_2 [18]. On the one hand, however, gold catalysts are normally supported on metal oxides such as TiO_2 [19–21], ZrO_2 [22], ZnO [23], Al_2O_3 [24] and SiO_2 [25] to keep them highly dispersed to prevent deactivation due to easiness of aggregation. On the other hand, recent work shows that CNTs may be a solution to overcome this problem [26], and a simple and selective procedure has been developed to confine gold particles inside CNTs [27]. With the above in mind, we carried out a study of H_2 dissociation on CNT supported gold clusters.

* Corresponding author. Tel.: +86 25 83593353; fax: +86 25 83686553.
E-mail address: zxchen@nju.edu.cn (Z.-X. Chen).

0920-5861/$ – see front matter © 2010 Elsevier B.V. All rights reserved.
doi:10.1016/j.cattod.2010.11.072

The whole paper is structured as follows. After this introduction and description of the models and computational details in Section 2, we first investigated the interaction of CNTs with a series of small gold clusters in Sections 3.1–3.2. In Section 3.3 we examined the H_2 adsorption and dissociation on the CNT supported gold clusters. Finally conclusions are given in Section 4.

2. Models and computational details

The one-dimension periodic CNT is simulated in a tetragonal box with lattice vectors *a* and *b* long enough to keep the inter-tube separation > 10 Å, and the optimized lengths of *c* vector are 12.83 and 12.32 Å containing 6 repeat units for zigzag (*n*, 0) (*n* = 9–13) and 5 repeat units for armchair (*m*, *m*) (*m* = 5–8) nanotubes, respectively. Containing 8 repeat units for CNT(9, 0) and 7 repeat units for CNT(6, 6) models are used for the study involving encapsulated linear Au_4 and Au_5 clusters to avoid the interaction of a gold cluster with those in the neighboring cells. In all the models, the nearest inter-cluster separation along the *c* direction is >5 Å.

All the calculations were performed using Vienna *ab initio* simulation package [28–30] (VASP) with GGA-PW91 functional [31] and projector-augmented wave (PAW) potentials [32,33]. Except for the calculations of isolated Au, Au_3 and Au_5 clusters, the spin-polarization effects on the total energies of Au–CNT(9, 0) complex are computed to be negligible ($\Delta E < 0.02$ eV). Energy cutoff (350 eV) and *k*-points ($1 \times 1 \times 6$) were validated by the evaluation of binding energy E_{ad} of Au monomer inside CNT(9, 0) to guarantee an accuracy of 0.02 eV. The binding energy is defined as $E_{ad} = E_{Au} + E_{CNT} - E_{Au-CNT}$, in which E_{Au}, E_{CNT} and E_{Au-CNT} are the energies of the gold cluster, carbon nanotube and the Au–CNT complex, respectively. We used the Methfessel–Paxton method with a smearing width of 0.2 eV. Geometry optimizations were stopped when the residual force on each atom is smaller than 0.03 eV/Å. The transition states (TSs) of H_2 dissociation were located by climbing-image nudged elastic band (cNEB) method [34,35] and confirmed by only one imaginary frequency corresponding to the forming and breaking of the H–H bond.

3. Results and discussion

3.1. Au_1–Au_5 encapsulated inside the CNTs

We first checked the binding energy of Au monomer interacting with the inner wall of nine CNTs of different diameters ranging from 6.78 to 10.86 Å (Fig. 1a). While all armchair (*m*, *m*) CNTs are metallic, the zigzag (*n*, 0) CNTs are either metallic (*n* = 9, 12) or semiconducting (*n* = 10, 11 and 13). It is notable from Fig. 1a that: (i) Au monomer interacts less strongly with the three semi-conducting zigzag CNTs than with the metallic CNTs, indicating that metallic properties favor the Au–CNT interaction. (ii) The interaction of Au_1 with the metallic CNTs increases first and then decreases with the increasing diameter of the tubes, and has a maximum at (6, 6). It should be mentioned that when the tube diameter is less than 7.15 Å as in (9, 0), Au monomer is located on the central axis of the CNT while beyond this value it sits off-center as in (10, 0) by 0.10 Å. In all the cases the nearest Au–CNT distance is longer than 3.6 Å, indicating that the interaction between Au monomer and the CNTs embodies less chemical bonding.

Bader charge analysis [36–38] reveals that the Au monomer is negatively charged in the CNTs, e.g. −0.40 and −0.42 au in (9, 0) and (6, 6), respectively (Table 1). The qualitative charge transfer from the inner wall of CNTs to Au_1 is consistent with charge difference density (CDD) plots (Fig. 2). We found that the binding energy is closely related to the calculated Bader charges on the Au atom (Fig. 1b). This result clearly demonstrates that the interaction of Au_1 with the tubes is mainly controlled by charge transfer.

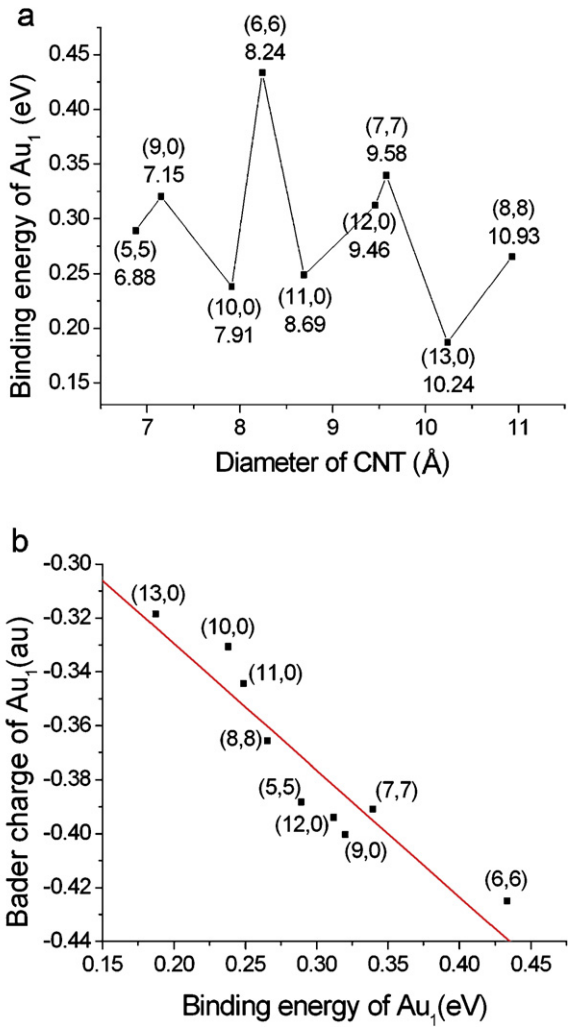

Fig. 1. (a) Binding energy (eV) of Au monomer encapsulated in the CNTs with increasing diameter (Å) of CNTs; (b) quasi-linear correlation between binding energy and Bader charge of the Au monomer encapsulated in the CNTs.

Table 1
Binding energy (E_{ad}, in eV), interaction energy (E_{int}, in eV), deformation energy (E_{def}, in eV) and Bader charges (*q*, in au) on Au_n clusters inside and outside the CNT(9, 0) and (6, 6).

		Inside		Outside	
		(9, 0)	(6, 6)	(9, 0)	(6, 6)
Au_1	E_{ad}	0.32	0.43	0.45	0.41
	E_{int}	0.32	0.43	0.72	0.67
	E_{def}	0.00	0.00	0.27	0.26
	q	−0.40	−0.42	−0.11	−0.14
Au_2	E_{ad}	−0.05	0.41	0.87	0.76
	E_{int}	−0.03	0.45	1.01	0.82
	E_{def}	0.02	0.04	0.14	0.06
	q	−0.06	−0.06	−0.06	−0.06
Au_3	E_{ad}	0.84	1.18	1.03	0.67
	E_{int}	0.95	1.38	1.64	0.71
	E_{def}	0.11	0.20	0.61	0.04
	q	−0.69	−0.82	0.05	−0.09
Au_4	E_{ad}	−0.31	0.33	1.16	0.81
	E_{int}	0.63	0.39	1.81	1.26
	E_{def}	0.94	0.06	0.65	0.45
	q	−0.77	−0.07	−0.03	−0.03
Au_5	E_{ad}	−0.59	0.25	1.13	0.72
	E_{int}	1.18	1.59	2.43	1.55
	E_{def}	1.77	1.34	1.30	0.83
	q	−0.62	−0.73	0.00	0.00

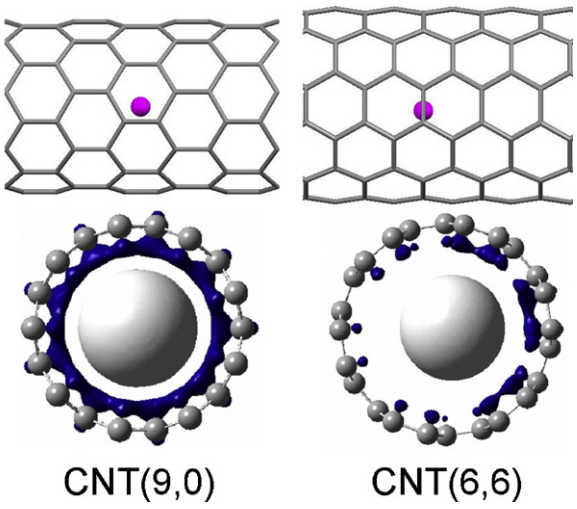

Fig. 2. Structure and charge difference density (CDD, $\rho_{CDD} = \rho_{Au-CNT} - (\rho_{Au} + \rho_{CNT})$) for Au monomer encapsulated in CNT(9, 0) and (6, 6). ρ_{CNT}, ρ_{Au} and ρ_{Au-CNT} refer to the total charge density of CNT, Au_1 and the Au_1–CNT complexes, respectively. White and dark blue denote accumulation and depletion, respectively. (For interpretation of the references to color in this figure legend, the reader is referred to the web version of the article.)

On the basis of the results of Au monomer, we choose CNT(9, 0) and (6, 6) that interact most strongly with Au monomer to investigate the interaction of zigzag and armchair CNTs with clusters Au_2–Au_5. The most stable adsorption structures and the CDD plots are shown in Fig. 3. For Au_2, the Au–Au bond is aligned along the central axis of the narrower CNT(9, 0), but normal to the axis in broader CNT(6, 6). The calculated binding energy is −0.05 eV in (9, 0) compared to a notably large value of 0.41 eV for (6, 6) (Table 1). The larger binding energy for (6, 6) than that for (9, 0) can be rationalized as follows. The dumbbell-like lowest unoccupied molecular orbital (LUMO) of Au_2 has a nodal plane normal to the Au–Au bond axis [39]. When Au_2 bond axis is parallel to the axis of a CNT as in (9, 0), the LUMO of Au_2 cannot effectively overlap with the MOs of the CNT. On the other hand, when the Au–Au bond is allowed to be vertical to the axis of a CNT like (6, 6), such overlap is favored because of symmetry adaptation. Our calculated Bader charges of the dimer are negligible in both (9, 0) and (6, 6), which is in agreement with the qualitative CDD of the complexes (Fig. 3).

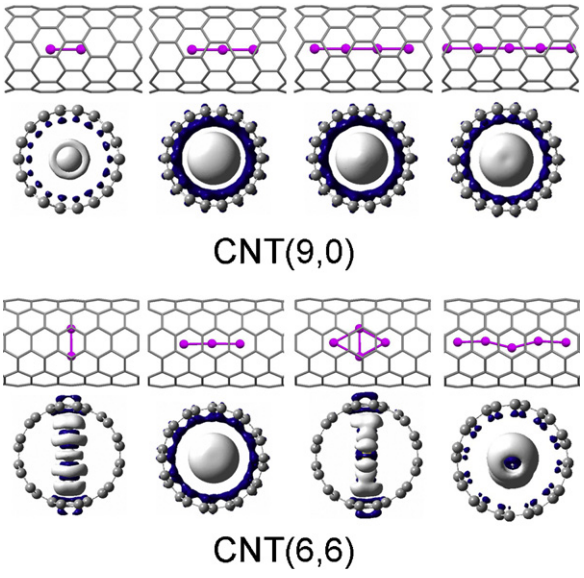

Fig. 3. The most favorable structures for encapsulation of Au_2–Au_5 in CNT(9, 0) and CNT(6, 6) and the charge difference density (CDD, $\rho_{CDD} = \rho_{Au-CNT} - (\rho_{Au} + \rho_{CNT})$) of the complexes. White and dark blue denote accumulation and depletion, respectively. (For interpretation of the references to color in this figure legend, the reader is referred to the web version of the article.)

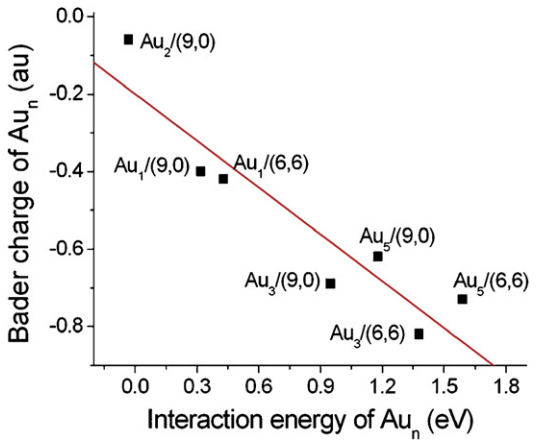

Fig. 4. Quasi-linear correlation between the interaction energy and the Bader charge of Au clusters encapsulated inside the CNT(9, 0) and (6, 6).

The most stable configurations of isolated Au_3, Au_4 and Au_5 are triangle, rhombus and "W" shapes, respectively [40,41]. Due to the limited space in CNTs, distortion of the cluster framework is necessary to stabilize the system. To quantitatively estimate the deformation, we defined the deformation energy $E_{def} = E_{int} - E_{ad}$. Here $E_{int} = E^*_{Au} + E^*_{CNT} - E_{Au-CNT}$, is the interaction energy which reflects the in situ binding strength [42] between a cluster and the CNT. E^*_{CNT} and E^*_{Au} are the energies of the CNT and cluster taking the geometries as in the corresponding complex, and E_{CNT-Au} is the total energy of the complex.

As can be seen in Table 1, Au_3 has the largest binding energy (0.84 and 1.18 eV) and interaction energy (0.95 and 1.38 eV), consistent with the large amount of charge transfer (−0.69 and −0.82 au) as well as the small deformation (0.11 and 0.20 eV) in (9, 0) and (6, 6), respectively. Au_4 is forced to be linear along the central axis of (9, 0) but retains its pristine rhombus skeleton in wider (6, 6). The calculated binding energy is 0.33 eV in (6, 6), compared to −0.35 eV in (9, 0) because of large deformation of the cluster in the latter. Au_5 displays linear/quasi-linear in (9, 0)/(6, 6) with a binding energy of −0.59/0.25 eV. Comparison of the calculated Bader charges and interaction energies reveals that there is a quasi-linear correlation between these two quantities except for Au_2 and Au_4 in (6, 6) and Au_4 in (9, 0) (Fig. 4). This finding again demonstrates that charge transfer plays an important role in the encapsulation interactions of gold clusters with the CNTs.

3.2. Au_1–Au_5 deposited outside the CNTs

In agreement with the recent report [43], Au monomer favors the top site of C atom on both (9, 0) and (6, 6) tubes (Fig. 5). Different from the encapsulation, the nearest Au–CNT distances are much shorter, being 2.21 and 2.23 Å, respectively, indicating an enhanced Au_1 and CNT interaction, which is in line with the calculated interaction energy, >0.65 eV for outside deposited Au monomer, compared to <0.45 eV for the encapsulated one (Table 1). Due to deformation of CNTs, the calculated binding energies, 0.45 eV for (9, 0) and 0.41 eV for (6, 6), is comparable to that for the encapsulated Au_1 (E_{ad} = 0.32 and 0.43 eV for (9, 0) and (6, 6), respectively).

Au_2 deposited outside the CNTs inclines to be vertical to the C–C bond (Fig. 5) with E_{ad} = 0.87 and 0.76 eV on (9, 0) and (6, 6), respectively and is more stable than the corresponding one inside

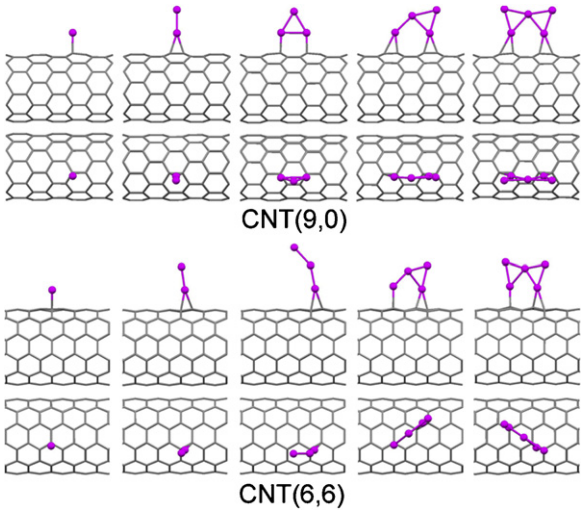

Fig. 5. The most favorable adsorption structures of Au clusters deposited on CNT(9, 0) and CNT (6, 6).

the tubes. Au_3 becomes a sharp triangle on CNT(9, 0) with two Au atoms binding to the carbon atoms on a hexagon diagonal. Such structure is more stable (E_{ad} = 1.03 eV) than the obtuse triangle (E_{ad} = 0.83 eV) with one side adsorbed on the CNT. On (6, 6) the obtuse triangle structure and the sharp one has essentially the same stability with the calculated binding energy being about 0.67 eV. Though Au_3/CNT(9, 0) deforms greatly with a deformation energy of 0.61 eV, a significant binding energy of 1.03 eV is calculated because of a stronger interaction (E_{int} = 1.64 eV) between Au_3 and CNT(9, 0) than that (0.71 eV) for CNT(6, 6). The structural difference of Au_3 on the zigzag (9, 0) and armchair (6, 6) may be due to the different potential energy surfaces on the CNT's outer surfaces induced by chirality and curvature [44]. For Au_4 and Au_5, one Au–Au bond is broken upon adsorption on the CNTs, which results in large deformations, i.e., 0.65 and 1.30 eV on (9, 0) and 0.45 and 0.83 eV on (6, 6) for Au_4 and Au_5, respectively. The different chiralities of the tubes lead to the different orientations of Au_4 and Au_5 (Fig. 5). Compared with encapsulation, Au_4 and Au_5 are much more stable adsorbed outside the tubes. The largest binding energy difference reaches 1.72 eV for Au_5/(9, 0). In fact, apart from Au_3 in (6, 6), clusters outside the CNTs possess larger values of E_{int} (Table 1) than the encapsulated clusters, indicative of stronger interaction in the former.

The charges on Au_1 atom are −0.11 and −0.14 au on (9, 0) and (6, 6), respectively, both of which are smaller than those inside the tubes (Table 1). Au_2–Au_5 clusters deposited outside of CNT(9, 0) and (6, 6) also possess negligible charges with an absolute value of less than 0.1 au. Therefore, charge transfer is no longer the main factor controlling the Au–CNT interaction when Au clusters are adsorbed outside the CNTs. Natural bond orbital [45] analyses with Gaussian 03 program [46] reveal that the main factor controlling the interaction between the outside deposited Au cluster and CNT is the donor–acceptor interaction between the 6 s AO(s) of Au atom(s) and the bonding π and anti-bonding π* orbitals of the C=C bond of the CNT.

3.3. H_2 dissociation by Au_n–CNT

Having studied the interaction of gold clusters with the CNTs, we now deal with dissociation of H_2 on these clusters. Figs. 6 and 7 depict the initial state (IS), transition state (TS) and final state (FS) structures for the process in and outside CNT(9, 0) and (6, 6) CNTs, respectively. The corresponding energetics and geometrical parameters are listed in Tables 2 and 3. Adsorption of H_2 molecule on gold

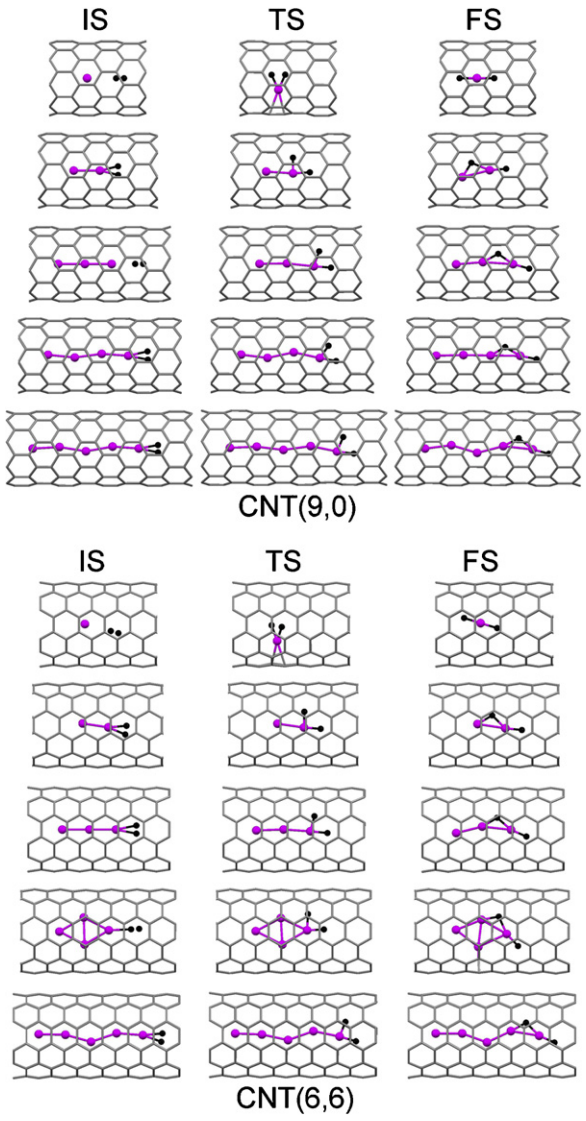

Fig. 6. Initial (IS), transition (TS) and final (FS) state structures for H_2 dissociation on Au clusters inside the CNT(9, 0) and (6, 6). Pink and black spheres refer to Au and H atoms, respectively. (For interpretation of the references to color in this figure legend, the reader is referred to the web version of the article.)

clusters exhibit two types of modes: in the first mode the H atoms and the bound Au form a linear structure while in the second the H atoms and the Au atom form a triangular structure. Adsorption of H_2 on encapsulated Au monomer, Au_3 in (9, 0) and Au_4 in (6, 6) belongs to the first mode. The remaining systems are of the second type. The first mode is generally less stable than the second one. For example, the H_2 binding energy is no more than 0.1 eV for the first mode whereas a largest binding energy of 0.58 eV is calculated for the second mode on Au_2 inside (9, 0). Because of the weaker interaction, the H–H bond, ~0.77 Å in the linear mode, is shorter than the one in triangular mode, >0.80 Å. Correspondingly the Au–H bond is longer in the linear mode than in the triangular mode. Different adsorption modes are ascribed to the different molecular orbitals used by H_2 to bind to clusters. In the triangular mode, the highest occupied molecular orbital of H_2 is used whereas in the linear structure H_2 employs its lowest unoccupied molecular orbital [42].

Let us first discuss H_2 dissociation on the gold clusters inside the CNTs. For the first mode the H–H bond in the ISs ranges from 0.76 to 0.78 Å (Table 2). In the TSs, the H–H bond extends to more than 1.7 Å except for Au_1 in (9, 0) for which a 1.32 Å is calculated.

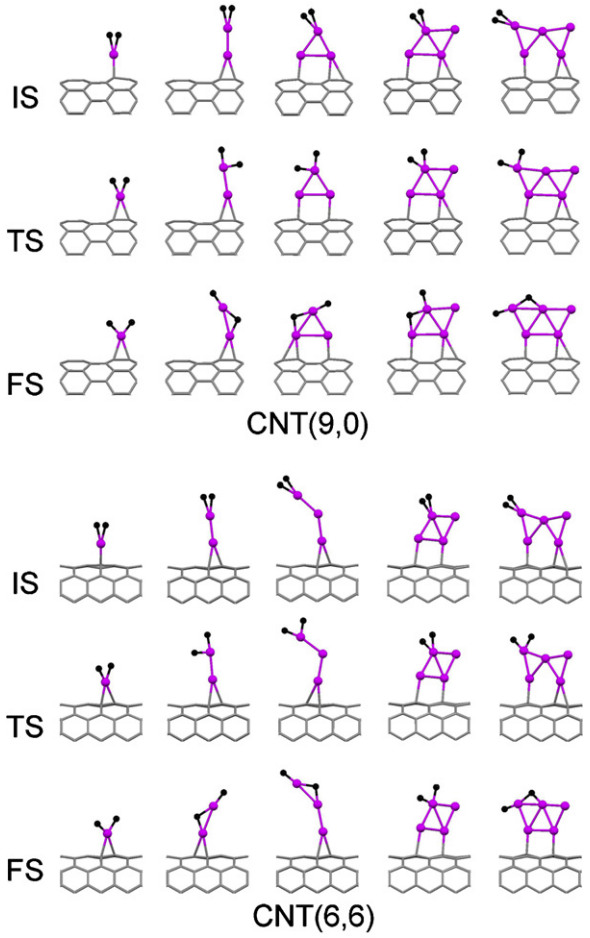

Fig. 7. Initial (IS), transition (TS) and final (FS) state structures for H_2 dissociation on Au clusters outside the CNT(9, 0) and (6, 6). Pink and black spheres refer to Au and H atoms, respectively. (For interpretation of the references to color in this figure legend, the reader is referred to the web version of the article.)

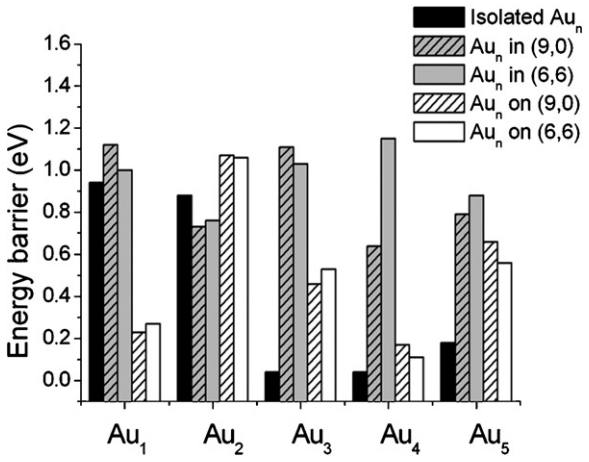

Fig. 8. Variation of energy barriers of H_2 dissociation on Au_n clusters in the isolated state and encapsulated inside or deposited outside the (9, 0) and (6, 6) tubes.

With the elongation of the H–H bond, the Au–H bond shrinks from >2.0 Å in the ISs to less than 1.60 Å in the TSs. In the FSs, the H–H bond length reaches more than 3.30 Å and the Au–H distance is about 1.7–1.8 Å (Table 2). The calculated barriers are higher than 1.0 eV. All the processes are exothermic, as evidenced by the calculated reaction heat from −0.29 to −1.90 eV. In the remaining six systems H_2 adsorption exhibits the triangular mode in which the H–H bond in the ISs, 0.79–0.85 Å, is longer than those in the linear mode. When the H–H bond elongates to 1.78–2.29 Å, transition states are reached. In the FSs these bonds extend to >3.0 Å. Because of stronger binding, the Au–H bonds, 1.78–2.01 Å, are shorter than those in the first mode. With the weakening of the H–H bond, the Au–H bond length decreases to about 1.55 Å in the TSs (Table 2). The barriers are between 0.64 eV [Au_4 in (9, 0)], and 1.03 eV [Au_3 in (6, 6)], which are lower than the values for the linear adsorption mode. This should be due to more activated H_2 (longer H–H bond) in the ISs, which makes the ISs less stable. Except for Au_2 in (6, 6), all the reactions are exothermic with the largest exothermicity of 0.61 eV for Au_3 in (6, 6).

Fig. 8 compares the computed barriers for H_2 dissociation on bare and supported gold clusters. It is clear that H_2 dissociation on CNT encapsulated gold clusters becomes more unfavorable than those on bare clusters except for Au_2 where a reduction of 0.13 eV is calculated. For example, on naked Au_3, the dissociation barrier is negligible, 0.04 eV. However, on the encapsulated Au_3, the barrier increases to more than 1.0 eV (Table 2).

Table 2
The binding energy of H_2 (E_{ad}, in eV), activation barrier (E_a, in eV) and reaction heat (E_r, in eV) for H_2 dissociation on Au_1–Au_5 clusters inside the CNT(9, 0) and (6, 6) and Au–H and H–H distances (d, in Å) in ISs, TSs and FSs.

Inside		E_{ad}	E_a	E_r	d_{H-H}			d_{Au-H}[b]		
					IS	TS	FS	IS	TS	FS
Au_1	(9, 0)	0.06	1.12	−0.34	0.76	1.32	3.34	2.80	1.59	1.67
	(6, 6)	0.10	1.00	−1.90	0.76	1.22	3.33	2.59	1.61	1.66
	Ref[a]	0.08	0.94	0.00	0.78	1.72	2.93	2.05	1.63	1.62
Au_2	(9, 0)	0.58	0.73	−0.04	0.84	2.17	3.40	1.80	1.54	1.89
	(6, 6)	0.40	0.76	0.05	0.85	2.29	3.19	1.78	1.55	1.78
	Ref.[a]	0.66	0.88	0.06	0.85	2.22	3.15	1.77	1.52	1.77
Au_3	(9, 0)	0.07	1.11	−0.48	0.77	1.95	3.31	2.27	1.54	1.74
	(6, 6)	0.10	1.03	−0.61	0.79	2.07	3.36	2.01	1.54	1.78
	Ref.[a]	0.78	0.04	0.01	0.90	1.29	1.91	1.72	1.60	1.57
Au_4	(9, 0)	0.07	0.64	−0.36	0.81	1.78	3.32	1.90	1.55	1.75
	(6, 6)	0.08	1.15	−0.29	0.78	2.14	3.39	2.08	1.57	1.83
	Ref.[a]	0.70	0.04	−0.09	0.90	1.27	2.11	1.73	1.60	1.57
Au_5	(9, 0)	0.29	0.79	−0.25	0.81	1.93	3.28	1.88	1.54	1.74
	(6, 6)	0.25	0.88	−0.43	0.82	2.15	3.34	1.89	1.54	1.79
	Ref.[a]	0.28	0.18	−0.24	0.84	1.35	2.61	1.82	1.59	1.82

[a] The data refer to the results on bare Au clusters from Ref. [42].
[b] The listed Au–H distance refers to that of the two shortest Au–H bonds.

Table 3
The binding energy of H_2 (E_{ad}, in eV), activation barrier (E_a, in eV) and reaction heat (E_r, in eV) for H_2 dissociation on Au_1–Au_5 clusters deposited outside the CNT(9, 0) and (6, 6) and Au–H and H–H distances (d, in Å) in ISs, TSs and FSs.

Outside		E_{ad}	E_a	E_r	d_{H-H}			d_{Au-H}[b]		
					IS	TS	FS	IS	TS	FS
Au_1	(9, 0)	0.16	0.23	0.10	0.82	1.40	2.07	1.86	1.61	1.61
	(6, 6)	0.11	0.27	0.06	0.81	1.25	2.11	1.87	1.61	1.61
	Ref.[a]	0.08	0.94	0.00	0.78	1.72	2.93	2.05	1.63	1.62
Au_2	(9, 0)	0.31	1.07	−0.15	0.81	2.17	3.36	1.89	1.52	1.78
	(6, 6)	0.35	1.06	−0.19	0.82	2.15	3.35	1.86	1.52	1.80
	Ref.[a]	0.66	0.88	0.06	0.85	2.22	3.15	1.77	1.52	1.77
Au_3	(9, 0)	0.10	0.46	−0.65	0.80	2.24	3.42	1.98	1.61	1.85
	(6, 6)	0.24	0.53	−0.28	0.82	2.00	3.28	1.86	1.56	1.79
	Ref.[a]	0.78	0.04	0.01	0.90	1.29	1.91	1.72	1.60	1.57
Au_4	(9, 0)	0.23	0.17	−0.09	0.84	1.46	2.43	1.85	1.60	1.71
	(6, 6)	0.24	0.11	−0.05	0.86	1.32	2.16	1.79	1.61	1.58
	Ref.[a]	0.70	0.04	−0.09	0.90	1.27	2.11	1.73	1.60	1.57
Au_5	(9, 0)	0.23	0.66	−0.12	0.81	2.20	3.40	1.89	1.57	1.82
	(6, 6)	0.25	0.56	−0.17	0.82	2.15	3.40	1.87	1.58	1.83
	Ref.[a]	0.28	0.18	−0.24	0.84	1.35	2.61	1.82	1.59	1.82

[a] The data refer to the results on bare Au clusters from Ref. [42].
[b] The listed Au–H distance refers to that of the two shortest Au–H bonds.

Previously we showed that negative charges are unfavorable for H_2 adsorption on isolated gold clusters [42]. Thus negatively charged Au_n clusters encapsulated inside the CNTs will interact less strongly with H_2 than the bare clusters do. Indeed, most binding energies for H_2 on the CNT supported clusters are smaller than results on the bare ones. For instance, the binding energy on Au_3, 0.78 eV, drops to around 0.1 eV (Table 2). The weak binding implies less activated H_2 as shown by the shorter H–H bond distance in the ISs. On naked Au_3, the H–H bond is 0.90 Å which is more than 0.1 Å longer than the values on the supported Au_3 (Table 2). Therefore, kinetically encapsulation of gold clusters into CNTs is not favorable for H_2 dissociation, though our calculated reaction heat demonstrates that thermodynamically dissociation is enhanced inside the CNTs (Table 2). This finding shows that the confinement effect may not be helpful for all types of reactions.

H_2 binds to the gold clusters outside CNTs via the triangular mode exclusively (Fig. 7). The H–H bond distance is around 0.8 Å which is shorter than the result for the corresponding unsupported clusters except for Au monomer because H_2 adsorbs on bare Au_1 in the linear mode. The binding energy is smaller compared to the situation on bare clusters (Table 3). Consistently the Au–H bond distance is longer for the supported clusters than for the bare ones. Depending on the system, the H–H bond distance in TSs ranges from 1.25 Å for Au_1 on (6, 6) to 2.24 Å for Au_3 on (9, 0) (Table 3). The variation of the H–H length is also remarkable in the FSs, with the maximum difference of 1.35 Å for Au_1 and Au_3 on (9, 0). The shortening of the Au–H contact is less than 0.4 Å from ISs to TSs.

Since H_2 generally interacts more strongly with the clusters outside the CNTs than with the encapsulated clusters, H_2 is more activated in the former. Therefore lower barriers are expected for H_2 dissociation on the outside deposited clusters. This expectation is consistent with the calculated barriers except for Au_2 (Fig. 8 and Tables 2 and 3). The abnormal behavior with Au_2 is in fact not inconsistent with the expectation because in this case the binding energy of H_2 on the encapsulated Au_2 is larger than the outside deposited Au dimer (Tables 2 and 3). One thing needs to be pointed out. There might be relatively higher partial pressure of H_2 in the inner cavity of CNT with respect to the external surface, which may modify the reactivity of confined nanoparticles. Compared with the bare Au_2–Au_5 clusters, the H_2 dissociation barriers on the deposited clusters are higher, indicating that the Au–CNT interaction hinders the process. However, a significant decrease of barrier, >0.6 eV, is computed on Au monomer deposited on the CNTs. This result may be due to the early transition state character of H_2 dissociation on Au monomer adsorbed outside the CNTs. In fact, a look at the data in Tables 2 and 3 shows that all the TSs can be classified into early and late transition states, based on the H–H bond distance in the TS. The early transition state normally has a H–H distance of about 1.3 Å while the late transition state is usually characterized with an H–H distance of ~2.0 Å. The former features a low barrier whereas the latter possesses relatively high barrier. This phenomenon can be rationalized as follows. Take the sum of the energy of Au_n/CNT and the energy of free H_2 as energy zero, the energy of a system M (M = IS, TS), ${}^{M}E$, can be approximated as ${}^{M}E = {}^{M}E_{H+H} + {}^{M}E_{H+H\text{-sub}}$. Here ${}^{M}E_{H+H}$ and ${}^{M}E_{H+H\text{-sub}}$ denote the interaction between H atoms and that between H atoms and the substrate (Au_n/CNT) in M system, respectively. The barrier E_a then is $({}^{TS}E_{H+H} - {}^{IS}E_{H+H}) + ({}^{TS}E_{H+H\text{-sub}} - {}^{IS}E_{H+H\text{-sub}})$. For the systems under study $({}^{TS}E_{H+H\text{-sub}} - {}^{IS}E_{H+H\text{-sub}})$ is similar in different systems. ${}^{IS}E_{H+H}$ is basically unchanged which is H_2 bonding energy. Thus, $E_a = {}^{TS}E_{H+H}$—constant. ${}^{TS}E_{H+H}$ is related to the nature of TSs. An early TS has more negative ${}^{TS}E_{H+H}$ because of shorter H–H distance. Hence a low/high barrier is computed for an early/late TS.

4. Conclusion

We have investigated the interaction of carbon nanotubes with Au_n (n = 1–5) clusters. Encapsulated inside the tubes, gold clusters interact with the tube via charge transfer from the inner sidewall to the clusters, resulting in negatively charged clusters. Hence, metallic CNTs wrap the gold clusters more tightly than the semiconducting counterparts. Clusters deposited outside the tubes are usually more stable than those encapsulated inside CNTs. H_2 generally binds to CNT supported gold clusters less strongly than to bare clusters, indicating that H_2 is less activated. Consistently H_2 dissociation is suppressed on CNT supported gold clusters except for Au monomer deposited outside the CNTs and Au dimer inside the CNTs. Our results demonstrate that CNT does not show positive effect for H_2 dissociation. Its promotion effect depends not only on the reaction but also on the size of catalysts. The present study further demonstrates that confinement effect is not effective for all types of reactions.

Acknowledgments

We greatly acknowledge the financial supports from the National Natural Science Foundation Grant Nos. 20573052 and 20973090 and 973 Programs 2009CB623504 and 2011CB808604 and the Scientific Research Foundation of Graduate School of Nanjing University (No. 2008CL06).

References

[1] P. Serp, M. Corrias, P. Kalck, Appl. Catal. A: Gen. 253 (2003) 337.
[2] C.A. Dyke, J.M. Tour, J. Phys. Chem. A 108 (2004) 11151.
[3] G.G. Wildgoose, C.E. Banks, R.G. Compton, Small 2 (2006) 182.
[4] H.X. Ma, L.C. Wang, L.Y. Chen, et al., Catal. Commun. 8 (2007) 452.
[5] W. Chen, Z.L. Fan, X.L. Pan, et al., J. Am. Chem. Soc. 130 (2008) 9414.
[6] X.L. Pan, Z.L. Fan, W. Chen, et al., Nat. Mater. 6 (2007) 507.
[7] A. Tavasoli, M. Trepanier, A.K. Dalai, et al., J. Chem. Eng. Data 55 (2010) 2757.
[8] M. Haruta, T. Kobayashi, H. Sano, et al., Chem. Lett. 16 (1987) 405.
[9] G.J. Hutchings, J. Catal. 96 (1985) 292.
[10] M. Haruta, S. Tsubota, T. Kobayashi, et al., J. Catal. 144 (1993) 175.
[11] G.C. Bond, D.T. Thompson, Catal. Rev. -Sci. Eng. 41 (1999) 319.
[12] M. Haruta, Cattech 6 (2002) 102.
[13] P. Claus, Appl. Catal. A: Gen. 291 (2005) 222.
[14] Q. Fu, H. Saltsburg, M. Flytzani-Stephanopoulos, Science 301 (2003) 935.
[15] T. Hayashi, K. Tanaka, M. Haruta, J. Catal. 178 (1998) 566.
[16] S. Biella, M. Rossi, Chem. Commun. (2003) 378.
[17] A. Abad, P. Concepcion, A. Corma, et al., Angew. Chem. Int. Ed. 44 (2005) 4066.
[18] J.K. Edwards, G.J. Hutchings, Angew. Chem. Int. Ed. 47 (2008) 9192.
[19] M.S. Chen, D.W. Goodman, Science 306 (2004) 252.
[20] P. Claus, A. Brückner, C. Mohr, et al., J. Am. Chem. Soc. 122 (2000) 11430.
[21] D.A. Panayotov, J.T. Yates Jr., J. Phys. Chem. C 111 (2007) 2959.
[22] C. Mohr, H. Hofmeister, P. Claus, J. Catal. 213 (2003) 86.
[23] C. Mohr, H. Hofmeister, J. Radnik, et al., J. Am. Chem. Soc. 125 (2003) 1905.
[24] E. Bus, J.T. Miller, J.A. van Bokhoven, J. Phys. Chem. B 109 (2005) 14581.
[25] C. Mohr, H. Hofmeister, M. Lucas, et al., Chem. Eng. Technol. 23 (2000) 324.
[26] X.H. Peng, J.Y. Chen, J.A. Misewich, et al., Chem. Soc. Rev. 38 (2009) 1076.
[27] P. Serp, E. Castillejos, ChemCatChem 2 (2010) 41.
[28] G. Kresse, J. Furthmüller, Phys. Rev. B 54 (1996) 11169.
[29] G. Kresse, J. Furthmüller, Comput. Mater. Sci. 6 (1996) 15.
[30] G. Kresse, J. Hafner, Phys. Rev. B 47 (1993) 558.
[31] J.P. Perdew, Y. Wang, Phys. Rev. B 45 (1992) 13244.
[32] P.E. Blöchl, Phys. Rev. B 50 (1994) 17953.
[33] G. Kresse, D. Joubert, Phys. Rev. B 59 (1999) 1758.
[34] G. Henkelman, B.P. Uberuaga, H. Jonsson, J. Chem. Phys. 113 (2000) 9901.
[35] D. Sheppard, R. Terrell, G. Henkelman, J. Chem. Phys. 128 (2008) 10.
[36] G. Henkelman, A. Arnaldsson, H. Jonsson, Comput. Mater. Sci. 36 (2006) 354.
[37] E. Sanville, S.D. Kenny, R. Smith, et al., J. Comput. Chem. 28 (2007) 899.
[38] W. Tang, E. Sanville, G. Henkelman, J. Phys. -Condens. Matter 21 (2009) 7.
[39] S. Chrétien, M.S. Gordon, H. Metiu, J. Chem. Phys. 121 (2004) 3756.
[40] X.B. Li, H.Y. Wang, X.D. Yang, et al., J. Chem. Phys. 126 (2007) 8.
[41] W. Fa, C.F. Luo, J.M. Dong, Phys. Rev. B 72 (2005) 4.
[42] G.-J. Kang, Z.-X. Chen, Z. Li, et al., J. Chem. Phys. 130 (2009) 034701.
[43] W. An, C.H. Turner, J. Phys. Chem. C 113 (2009) 7069.
[44] D.H. Seo, H.Y. Kim, J.H. Ryu, et al., J. Phys. Chem. C 113 (2009) 10416.
[45] E.D. Glendening, J.K. Badenhoop, A.E. Reed, et al., NBO 5.0, Theoretical Chemistry Institute, University of Wisconsin, Madison, 2001.
[46] M.J. Frisch, G.W. Trucks, H.B. Schlegel, et al., Gaussian 03, Revision D.01, Gaussian, Inc., Wallingford, CT, 2004.